Effects of Phenylalanine on the Liquid-Expanded and Liquid-Condensed States of Phosphatidylcholine Monolayers

Andrea C Cutro, E Anibal Disalvo and María A Frías

Applied Biophysics and Food Research Center, Centro de Investigaciones en Biofísica Aplicada y Alimentos (CIBAAL), National University of Santiago del Estero and CONICET, Santiago del Estero, Argentina.

ABSTRACT

BACKGROUND: Phenylalanine (Phe) is involved in physiological and pathological processes in cell membranes in which expanded and condensed states coexist. In this direction, it was reported that surface hydration is important for the binding affinity of the amino acid which significantly perturbs 1,2-dipalmitoyl-*sn*-glycero-3-phosphocholine (DPPC) monolayer structure and morphology. A deeper insight showed that Phe inserts in DPPC monolayer defects as a monomer at pH 5 and forms aggregates that adsorb to the membrane surface generating a reconfiguration of the lipid arrangement in areas of higher packing. This new arrangement in the monolayer causes the reorientation of dipoles of lipid and water molecules which is congruent with the dehydration and surface tension changes reported above. With this background, this article studies the affinity of Phe in liquid-expanded 1,2-dimyristoyl-*sn*-glycero-3 phosphocholine (LE DMPC) and liquid-condensed 1,2-dipalmitoyl-*sn*-glycero-3-phosphocholine (LC DPPC) monolayers and their effects on membrane properties.

RESULTS: The adsorption of Phe can be described by a cooperative process in non-independent sites suggesting that Phe/lipid systems reorganize to form new structures at a high degree of coverage. Compressibility modulus and Brewster angle microscopy (BAM) images allow to propose that Phe causes a new phase in 1,2-dimyristoyl-*sn*-glycero-3 phosphocholine (DMPC) and DPPC.

CONCLUSIONS: Phe imposes new arrangements in the lipid phase to form new structures with different compressibility behavior than lipid binary mixtures of DMPC and DPPC. Phe interaction with the LC and LE phases gives place to a process in which a synergistic effect between non-independent sites can be produced. These features of Phe/lipid interaction would be of great importance to understand the multiple effects of Phe on cell membranes.

KEYWORDS: DMPC, DPPC, monolayers, phenylalanine, compressibility, domains

Introduction

The understanding of the effects of phenylalanine (Phe) on cytotoxicity and cell deformation has encouraged several studies with model phospholipid-water interfaces mimicking the characteristic of cell membranes to gain insight into the molecular-level interactions.[1,2] Indeed, Phe produces leakage and membrane fusion of liposomes of phosphatidylcholine, phosphatidylethanolamine, and galactolipids.[3]

Phe residues have been identified as a key component in the formation of amyloid structures under pathologically relevant concentrations associated with a diverse group of diseases such as Alzheimer, type II diabetes, and prion disorders.[4] Furthermore, it was reported by Do et al[5] that there were favorable interactions between the cell membrane and the exterior (hydrophobic) which contribute to the cytotoxicity of Phe fibrils. A possible mechanism suggests that insertion in the membrane produces dehydration and phase changes.[6,7] In this direction, it was reported that surface hydration is important for the binding affinity and the amino acid-lipid interaction.[8] The effect of Phe on membrane hydration seems to alter considerably the interfacial tension and the surface domain

morphology of 1,2-dipalmitoyl-*sn*-glycero-3-phosphocholine (DPPC) films.[2,9] Perkins and colleagues[2,10] among others showed by a combination of surface-sensitive experimental techniques and molecular dynamics (MD) simulations that L-phenylalanine significantly perturbs DPPC monolayer structure and morphology. A deeper insight into these questions, reported recently by Cutro et al,[11] showed that Phe inserts in DPPC monolayer defects as a monomer at pH 5. Instead, at pH 7.3, it forms aggregates that adsorb to the membrane surface generating a reconfiguration of the lipid arrangement in areas of higher packing. This new arrangement in the monolayer causes the reorientation of dipoles of lipid and water molecules which is congruent with the dehydration and surface tension changes reported above.[12]

The Phe/DPPC dissociation constant, measured at pH 5 is $2.23 \pm 0.09\,mM$ from which the free energy change corresponding to the association is about $-3.615\,kcal/mol$ at $25°C$. The negative value of free energy suggests that the stabilization of Phe in the lipid interface may have enthalpic and entropic contributions.[13] The enthalpic contribution may correspond to hydrogen bonding which is supported by Fourier-transform

infrared (FTIR) spectroscopy data showing a decrease in the symmetric stretching frequency of the phosphate groups ($\nu_{sym}PO_2^-$) of the DPPC bilayers.[3,7] The entropic contribution may be ascribed to hydrophobic interaction that disrupts the water network around the phenyl group in the membrane defect. As Phe is rather hydrophilic (log P = −1.38) and highly soluble in water (log S = −0.788) at 25°C,[14] partition and accommodation of the hydrophobic phenyl ring at the interface of lipid membranes may depend on the phase state and hydration of the lipids. Under theoretical considerations, amino acids accumulate at the boundary between lipid domains.[15] The boundaries in a monolayer of one lipid species can be changed modulating the expanded and condensed phases by a mobile barrier.[16] Expanded and condensed monolayers contain different ratios of hydration and confined waters distributed along the different chemical groups of the phospholipids.[12,17,18] At a pressure of around 20 to 30 mN/m or lower, lipid interfaces include water molecules beyond the hydration shell. These highly structured water-arrangement-facing non-polar regions make them labile to biological effectors due to its high free energy accumulation (surface tension). This is related to the exposure of hydrophobic regions at low pressures. The water beyond the first hydration shell appears at surface pressures below the critical one in a $\Delta\pi/\pi$ curve.[19,20] It is concluded that the membrane surface is reactive to effectors such as amino acids when confined water, most probably organized in the adjacencies of acyl chains, is present. The observation that Phe blocks hydrophobic defects induced by dehydration favors the interpretation that this amino acid requires vacancies in which water exclusion may be produced.[13]

Expanded lipid interphases are then responsive to amino acids and peptide challenge. This is to say that amino acids can produce a further increase in surface pressure, that is, a decrease in surface tension, provided that they may find regions of organized water at the interphase. Phe is involved in physiological and pathological processes in cell membranes in which expanded and condensed states coexist.[21,22] Therefore, the aim of this article is to analyze the response to Phe of lipid monolayers at those different surface states. Structural changes produced in each different state of packing were analyzed by means of surface pressure-area per molecule isotherms and Brewster angle microscopy (BAM).

Materials and Methods

DPPC (>99% purity) and 1,2-dimyristoyl-*sn*-glycero-3 phosphocholine (DMPC; >99% purity) were purchased from Avanti Polar Lipids, Inc (Alabaster, AL). Phe was purchased from Sigma-Aldrich, Saint Louis (MO) (99% purity). Purity of lipids and Phe was checked by FTIR and ultraviolet (UV) spectroscopies (Figure S1—Supplementary Information). Chloroform from Merck was of spectroscopic quality.

Fresh stock solutions of Phe were prepared immediately before being used to avoid fiber formation.[11] The final concentration of stock solutions of pure lipids (DPPC and DMPC) was 4 mM in all the assays. Lipid mixtures of 1:9 and 9:1 DMPC/DPPC were assayed and prepared with adequate aliquots of the preformed chloroform solutions of pure lipids. All aqueous solutions were prepared with ultrapure water obtained from an Osmion reverse osmosis system containing 2 carbon and 2 ion-exchange columns. Then, water was purified through a 0.22-μm Zetapor filter. The resistivity of the purified water was 18 MΩ cm. During all the assays, temperature was maintained constant at 20°C ± 0.2°C for DPPC (liquid condensed [LC]), 33°C ± 0.2°C for DMPC (liquid expanded [LE]), and 31°C ± 0.2°C for the mixture of DMPC/DPPC (LC/LE) with a Cole-Parmer Polystat equipment and the final pH was 5.0.

Surface pressure change at constant area

Changes in the surface pressure of lipid monolayers upon the addition of Phe into the subphase were determined at constant area and temperature, in a Kibron μTrough S equipment. The total area of the interface was 1334 mm².

A chloroform solution of lipids was spread on the surface of 8 mL of 1 mM KCl at pH 5 to reach the surface pressure (π_0) of 14 ± 1 mN/m where the major changes were observed. Then, aliquots of Phe aqueous solution (160 mM) were injected in the subphase with permanent stirring. The changes produced in the surface pressure were registered as a function of time, until a constant value was reached as indicated in Figure S2—Supplementary Information. Data were collected after 15 minutes when the values were stable to avoid uncertainties due to perturbations during the injection.

Langmuir trough measurements

Surface pressure-area/molecule (π-A) isotherms were obtained by a KSV NIMA LB trough (area = 240.00 cm²) using a Pt Wilhelmy plate (39.24 mm²) as a sensor of surface pressure. Lipids in chloroform were spread over the aqueous solution using a Hamilton microsyringe with a precision of ±0.01 μL. Compression was performed with 2 barriers moving at the same speed (3.5 cm²/min). The reported π-A isotherms correspond to an average of at least 3 independent assays. Temperature was controlled with a precision within ±0.5°C.

Brewster angle microscopy

Langmuir monolayers were prepared on a Langmuir equipment mounted on the stage of a Nanofilm EP3 Imaging Ellipsometer (Accurion, Gottingen, Germany), which was used in the BAM mode. Minimum reflection was set with a polarized laser (λ = 532 nm) incident on the bare aqueous surface at the experimentally calibrated Brewster angle (~53.1°). The lipid monolayers were spread onto the aqueous surface and compressed to the specific pressure. The reflected light was collected through a 20× objective and an analyzer-polarized lens to a charge-coupled device (CCD) camera. The gray level at

each pixel of the BAM images can be converted to reflectivity values after the calibration factors were tested for each individual experiment.[23,24] The reflectivity obtained from BAM measures is related to the film thickness and to the refraction index of the film.[25,26]

Determination of the degree of coverage and affinity constant

The degree of coverage (q) can be calculated from the surface pressure changes induced by each Phe concentration in the subphase considering the equilibrium between the amino acid in the solution [Phe] in contact with the membrane M and amino acids adsorbed to it $[MPhe_n]$

$$M + n\mathrm{Phe} \Leftrightarrow MPhe_n$$
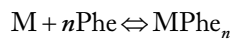
where "n" is the moles of Phe adsorbed to the membrane M.

At equilibrium, the velocity of adsorption

$$v_a = k_1(1-\theta)\left[\mathrm{Phe}\right]^n$$

is equal to the velocity of desorption

$$v_d = k_2\theta$$

where $(1-\theta)$ is the number of unoccupied sites in the membrane, k_1 the specific rate constant of adsorption, θ the number of occupied sites in the membrane, and k_2 is the specific rate constant of desorption.

Thus

$$k_1\left(1-\theta\right)\left[\mathrm{Phe}\right]^n = \theta k_2$$

from where equation (1) is obtained

$$\frac{\left[\mathrm{Phe}\right]^n}{\left(K_{\mathrm{dapp}} + \left[\mathrm{Phe}\right]^n\right)} = \theta \tag{1}$$

where $K_{\mathrm{dapp}} = k_2/k_1$ is the apparent dissociation constant for Phe in a given monolayer.

Experimentally, θ can be obtained from the surface pressure data by

$$\theta = \frac{\left(\pi - \pi_0\right)}{\left(\pi_\infty - \pi_0\right)} \tag{2}$$

where π is the surface pressure at each Phe concentration, π_0 is the initial surface pressure of the monolayer equilibrated before the addition of the amino acid to the subphase, and $\pi\infty$ is the surface pressure value reached after equilibration for a given Phe concentration. As observed when $\pi = \pi_0$, $\theta = 0$ (that is, no site is occupied). When $\pi = \pi\infty$, $\theta = 1$, meaning that all sites are occupied.

Combining equations (1) and (2), the isotherm is obtained

$$\theta = \frac{\pi - \pi_0}{\pi_{\max} - \pi_0} = \frac{\left[\mathrm{Phe}\right]^n}{K_{\mathrm{dapp}} + \left[\mathrm{Phe}\right]^n} \tag{3}$$

Equation (3) fits to a Langmuir adsorption isotherm when $n = 1$. A Langmuir adsorption isotherm corresponds to adsorption on independent sites on the surface meaning that the energy of interaction is independent of the degree of occupancy.[27] When data depart from the hyperbolic curve, they may be fitted to values of $n > 1$ which is interpreted as a consequence of structural changes produced by the adsorbate in the occupancy of the sites. This means that at different degrees of coverage the energy of interaction varies. In other words, sites are not independent because the occupancy of some of them affects the structure of the unoccupied ones. This cooperativity has also been applied to explain the allosteric phenomena in enzyme kinetics, which is a deviation from the Michaelis-Menten equation that has the same form than a Langmuir adsorption isotherm.[28]

Results

As shown in Figure 1A, the presence of increasing concentrations of Phe in the subphase of LE DMPC and LC DPPC monolayers stabilized at a surface pressure (π_0) of 14 mN/m causes a surface pressure increase in DMPC (red symbols) twice higher in comparison to DPPC (black symbols). These surface pressure increments are accompanied by morphological changes in DPPC (a and b) and DMPC (c and d) monolayers with the Phe addition according to BAM images.

The degree of coverage/Phe concentration isotherm, obtained from changes in surface pressure as described by equation (3) in section "Materials and Methods" can be fitted to calculate the dissociation constants of Phe for LE DMPC ($K_D = 21.93 \pm 1.65$) and for LC DPPC ($K_D = 32.31 \pm 7.60$) (Figure 1B).

Thus, the affinity of Phe is higher in DMPC in the LE state. Curves fit with $n = 1.53$ and $n = 1.62$ for DMPC and DPPC, which denotes a cooperative process in non-independent sites (see section "Materials and Methods"). This means that Phe/lipid systems reorganize to form new structures at a high degree of coverage as shown by BAM images in Figure 1A.

DMPC and DPPC surface pressure/area per molecule isotherms at $33°C \pm 0.2°C$ and $20°C \pm 0.2°C$ were analyzed at increasing concentrations of Phe (Figure 2A and B). In these conditions, DMPC monolayers are above the critical point of coexistence of the LE and LC states along the whole range of surface pressure, whereas the DPPC ones are below the critical point as shown by the defined plateau.

In Figure 2A, it is observed that the curve corresponding to DMPC in the LE state shifts to higher areas in the presence of increasing Phe concentrations. This is congruent with the observation that at a constant area Phe increases the surface pressure as shown in Figure 1A denoting its intercalation in the interphase.

For DPPC, at area values corresponding to the plateau at which the LE and LC states coexist, the curves shift to higher pressures (Figure 2B). However, at lower areas, in which the monolayer reaches the LC region, curves are shifted to lower
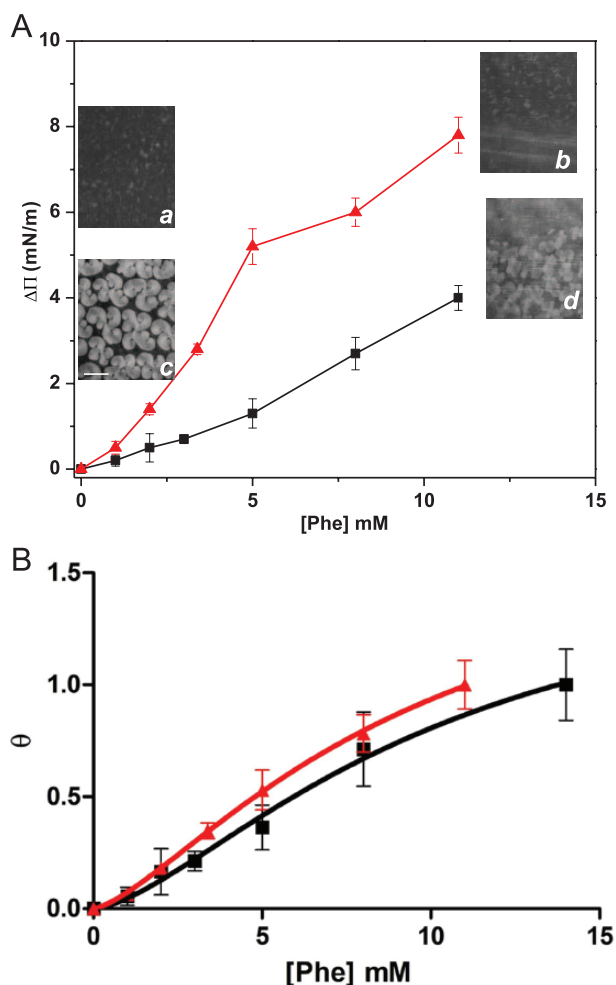
Figure 1. (A) Response in surface pressure to Phe concentration of monolayers at 14 mN/m for DMPC at 33°C (▲) and DPPC (■) at 20°C. BAM images—insets: (a) pure DMPC, (b) DMPC with 11 mM Phe, (c) pure DPPC, and (d) DPPC with 11 mM Phe (scale bar corresponds to 50 mm). (B) Degree of coverage (θ) of DMPC (▲) and DPPC (■) monolayers as a function of Phe concentration in the subphase at the initial pressure of 14 mN/m.
DMPC, 1,2-dimyristoyl-*sn*-glycero-3 phosphocholine; BAM, Brewster angle microscopy; DPPC, 1,2-dipalmitoyl-*sn*-glycero-3-phosphocholine.
Errors are reported as standard deviations of 3 different batches of lipid preparations and averaged.

Figure 2. (A) Surface pressure vs area per molecule isotherms for DMPC monolayer at 33°C ± 0.2°C on subphases without Phe (black curve), 2.5 mM Phe (light gray curve), 5 mM Phe (blue curve), and 11 mM Phe (red curve). (B) Surface pressure vs area per molecule isotherms for DPPC monolayers at 20°C ± 0.2°C on subphases without Phe (black solid line), 2.5 mM Phe (light gray curve), 5 mM Phe (blue curve), and 11 mM Phe (red curve).
DMPC, 1,2-dimyristoyl-*sn*-glycero-3 phosphocholine; DPPC, 1,2-dipalmitoyl-*sn*-glycero-3-phosphocholine.

pressures for concentrations of Phe between 2.5 and 5.0 mM. That is, at constant large areas, the behavior of the DPPC monolayer is qualitatively similar to that found for LE DMPC. However, at low areas, the surface pressure changes are, although to a lower extent, opposite to those at higher areas. This denotes that Phe effects are dependent on whether the monolayer is in the LE or LC state as shown in Figure 1 congruent with the differences found in the affinity of this amino acid for the different phase states.

The isotherm of LE DMPC in the presence of 11 mM Phe insinuates a slight shoulder at 150 Å² areas that is absent in pure DMPC monolayers in the same conditions (Figure 2A). In contrast, the most noticeable effect of Phe is that in DPP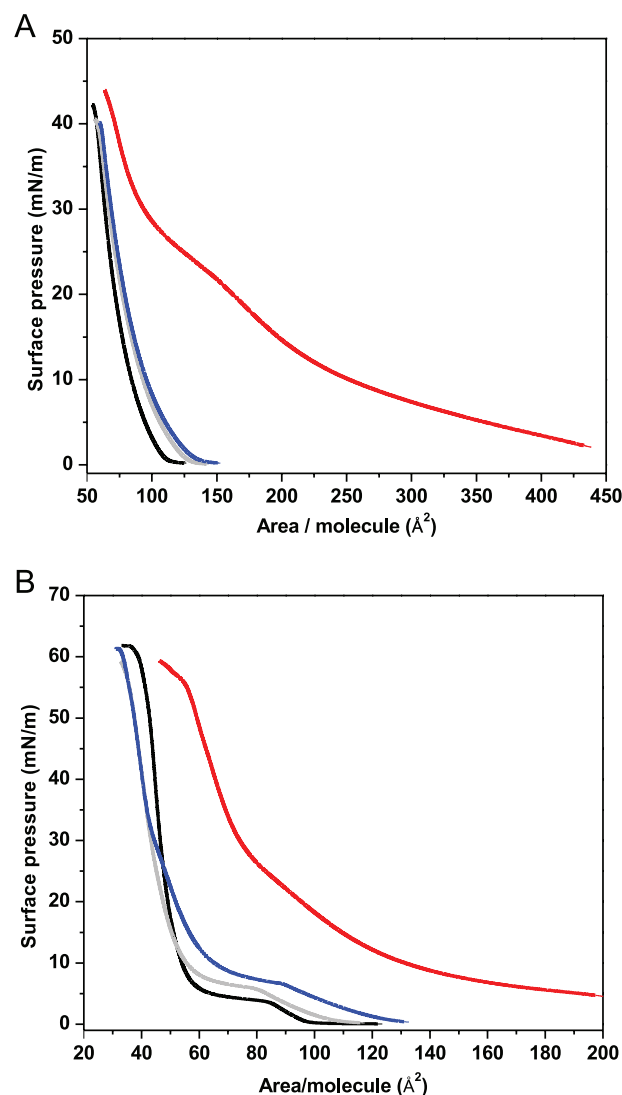C monolayers the characteristic LE–LC coexistence region commonly observed in DPPC π–A isotherm disappears in the presence of 11 mM Phe (Figure 2B) giving also a slight shoulder at 100 Å².

Figure 2A and B indicates that Phe produces opposed effects on membranes in the LE and LC phase states, as a result of which the compression properties of 11 mM Phe/DMPC and 11 mM Phe/DPPC are comparable in spite of the strong different initial states of the lipid interphases (see red lines in both figures).

The mixtures of Phe/DMPC and Phe/DPPC resemble the behavior of the mixtures of saturated and unsaturated lipids as reported to occur in DPPC/DOPC mixtures.[29] In this case,
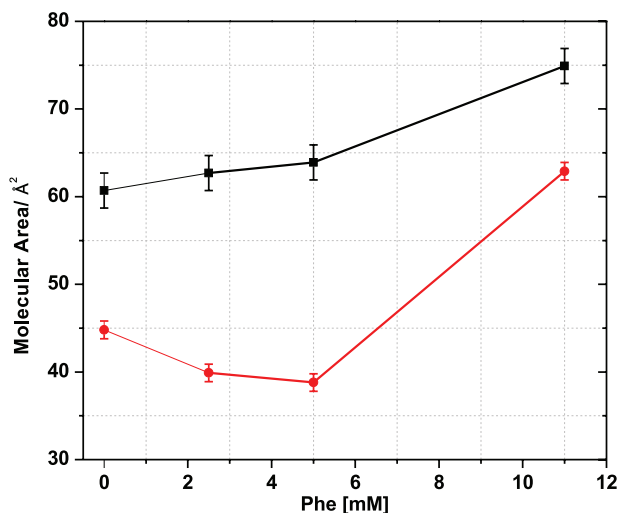
Figure 3. Changes in molecular area vs increasing concentrations of Phe in the subphase for DMPC (●) and DPPC (■) monolayers. DMPC, 1,2-dimyristoyl-*sn*-glycero-3 phosphocholine; DPPC, 1,2-dipalmitoyl-*sn*-glycero-3-phosphocholine.

the plateau appearing in DPPC monolayers below the critical point corresponding to the coexistence of the LE and LC phases tends to disappear with the increase in the DOPC ratio. The presence of 11 mM Phe in the subphase of DPPC monolayers in the LC state produces the same effect than increasing the molar fraction of DOPC in DPPC.

On the other way, Phe in the subphase of DMPC monolayers at a temperature at which there is no condensation (ie, above the critical point) shows an attenuated plateau. From the serial curves shown in Figure 2, the effect of Phe on the area per lipid can be derived (Figure 3). In the expanded phase of DMPC, Phe increases the area even at low concentrations at a constant surface pressure of 14 mN/m (Figure 3, black symbols). On the other hand, when Phe is added to condensed DPPC, the area decreases below 4 to 5 mM Phe and increases significantly above 5 mM (Figure 3, red symbols). The slight area decrease may be due to Phe insertion in vacancies (packing defects) present in the LC phase[11] that may reduce the repulsion between head groups producing a local contraction. When those vacancies are occupied, above 5 mM Phe appears to induce an area increase.

To visualize the phase properties of Phe/DMPC and Phe/DPPC systems, the compressibility module was calculated from the data in Figure 2A and B using equation (4)[30]

$$C^{-1} = -A \left(\frac{d\pi}{dA} \right)_T \qquad (4)$$

The compressibility modulus vs area/molecule is a quantitative measure of the state of the monolayer that indicates the occurrence of a change in the physical state, such as the coexistence of expanded-condensed phases in the film.[31]

For example, the compressibility curve for DPPC at a temperature below the phase transition gives 2 clear peaks: one centered at 45 Å[2] and a lower one at 90 Å[2] (Figure 4B, black
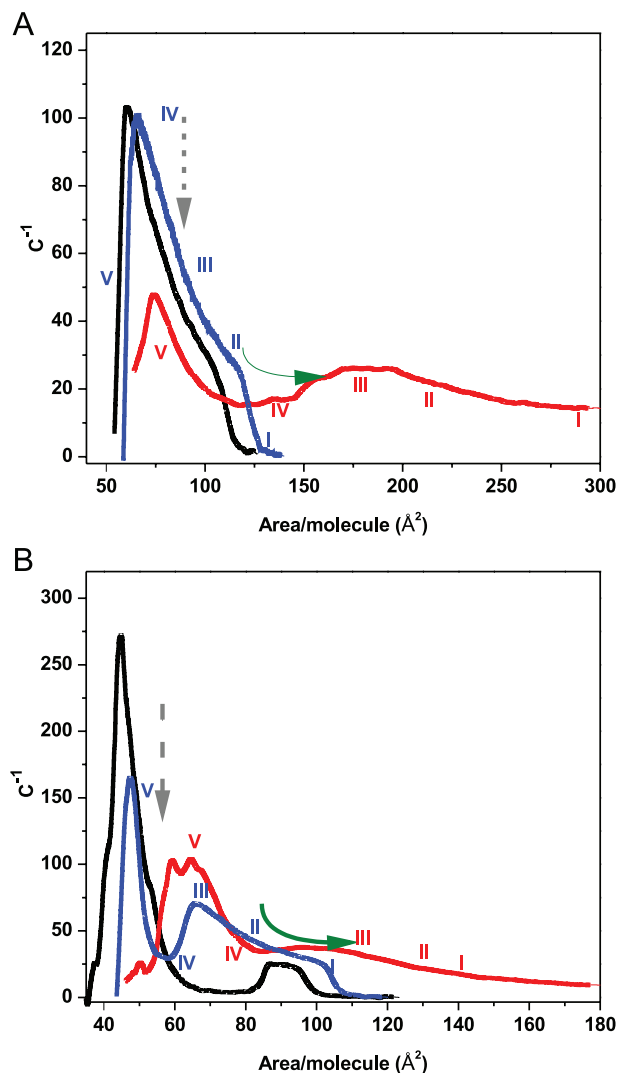

Figure 4. Compressibility module curves of (A) DMPC monolayer on water (black solid line), on 11 mM Phe (red solid line), and for a 9:1 DMPC/DPPC mixture (blue solid line) at 31°C. (B) DPPC on water (black solid line) at 20°C, on 11 mM Phe (red solid line) at 20°C, and for a 1:9 DMPC/DPPC mixture (blue solid line) at 31°C.
DMPC, 1,2-dimyristoyl-*sn*-glycero-3 phosphocholine; DPPC, 1,2-dipalmitoyl-*sn*-glycero-3-phosphocholine.

line). The positions of these peaks are coincident with the beginning and end of the flat region in which the surface pressure remains constant ascribed to the LC/LE phase coexistence (Figure 2B, black line).

The compressibility curves of DMPC show a peak at 60 Å[2] and a shoulder to higher areas approximately 10 Å[2] (Figure 4A, black line). The principal peak decreases in parallel to the appearance of a broad peak at higher areas with the addition of increasing amounts of Phe (Figure S3—Supplementary Information). On the other hand, the curves of DPPC show also a decrease of the principal peak with a deformation and broadening of the peak at higher areas with increasing Phe concentration (Figure S4—Supplementary Information). Although displaced to higher areas, the profile of 11 mM Phe/DMPC is qualitatively similar to that found for DPPC below
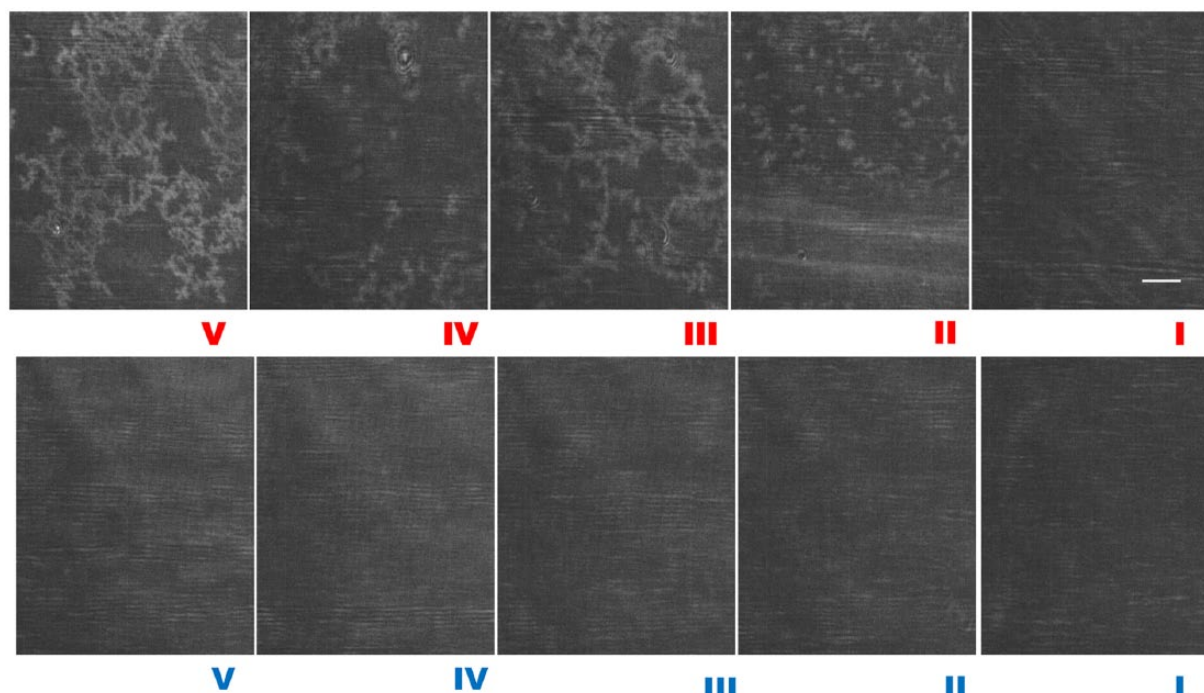
Figure 5. BAM images along compressibility for DMPC 11 mM Phe (upper panel) and a mixture of 9:1 DMPC/DPPC (lower panel) (scale bar corresponds to 50 mm). Number corresponds to the peaks shown in Figure 4A.

DMPC, 1,2-dimyristoyl-*sn*-glycero-3 phosphocholine; BAM, Brewster angle microscopy; DPPC, 1,2-dipalmitoyl-*sn*-glycero-3-phosphocholine.

the phase transition (Figure 4A, red line and Figure 4B, black line). In addition, Phe in DPPC gel state produces a profile in which the 2 peaks of DPPC (Figure 4B, black line) give place to a peak and a shoulder as observed for pure DMPC above the phase transition (Figure 4B, red line and Figure 4A, black line) also displaced to higher areas.

The comparison of red line curves in Figure 2A and B indicates that the compression profiles for the Phe/DMPC and Phe/DPPC mixtures are similar, in spite of the fact that in one case Phe is added to a system in the LE state and in the other in the LC ones. For this reason, DMPC/DPPC lipid mixtures at temperatures at which one lipid (DMPC) is in the LE state and the other (DPPC) is in the LC state without Phe were used to compare and elucidate a model of interaction depending on the monolayer state.

The analysis of DMPC monolayers doped with 10% DPPC is shown in Figure 4A (blue line). The green arrow indicates the displacement of the shoulder in pure DMPC to larger areas and the grey one the decrease of the peak at 60 Å^2 approximately, due to Phe. However, this displacement is not observed when DMPC is doped with 10% DPPC.

In Figure 4B, it is observed that the DPPC curve (black line) shows the 2 well-defined populations at 45 and 90 Å^2 with a profile similar to that for DPPC doped with 10% DMPC mixture (blue line), although the peak at higher areas is displaced. Thus, the effect of Phe on the phase state of LE-DMPC and LC-DPPC is of a different nature than that caused by the addition of lipids in the LC or LE state, respectively.

According to the BAM images, the increases in the surface pressure are accompanied by changes in the morphological

features of DPPC (Figure 1A and B) and DMPC (Figure 1C and D) monolayers with the subsequent aliquots of Phe added to the subphase. Changes are more noticeable in LC-DPPC than in LE-DMPC as derived from the C^{-1} analysis in Figure 4. In the upper panel of Figure 5 (red numbers), the presence of Phe in LE-DMPC monolayers at low pressures and large areas (Image II) promotes the appearance of regions that are not observed when DMPC is doped with 10% DPPC (lower panel; blue numbers). Congruently with compressibility curves, BAM images confirm that Phe interaction is different than that promoted by the addition of DPPC.

In contrast, the compression of DPPC in the presence of Phe (Figure 6, upper panel) produces less defined regions in comparison with DPPC with 10% DMPC (Figure 6, lower panel) which confirm the conclusions derived from the compressibility curves of Figure 4B.

It has already been shown with X-ray diffraction measurements[32] that in certain phases of floating fatty acid monolayers the molecules are tilted with respect to the normal axis of the surface. This observation may result in an optical anisotropy of the monolayer depending on the orientation of the tilted molecules.[33] Thus, the morphological change in Figures 5 and 6 has been ascribed to distinct molecular orientation in each of the 2 coexisting phases.[32,33]

Discussion

The interaction of Phe with DMPC in the LE and with DPPC in the LC state takes place in at least 2 steps: adsorption and reorganization of the lipid matrix as it is inferred by the values of $n > 1$, calculated from curves shown in Figure 1B. The final
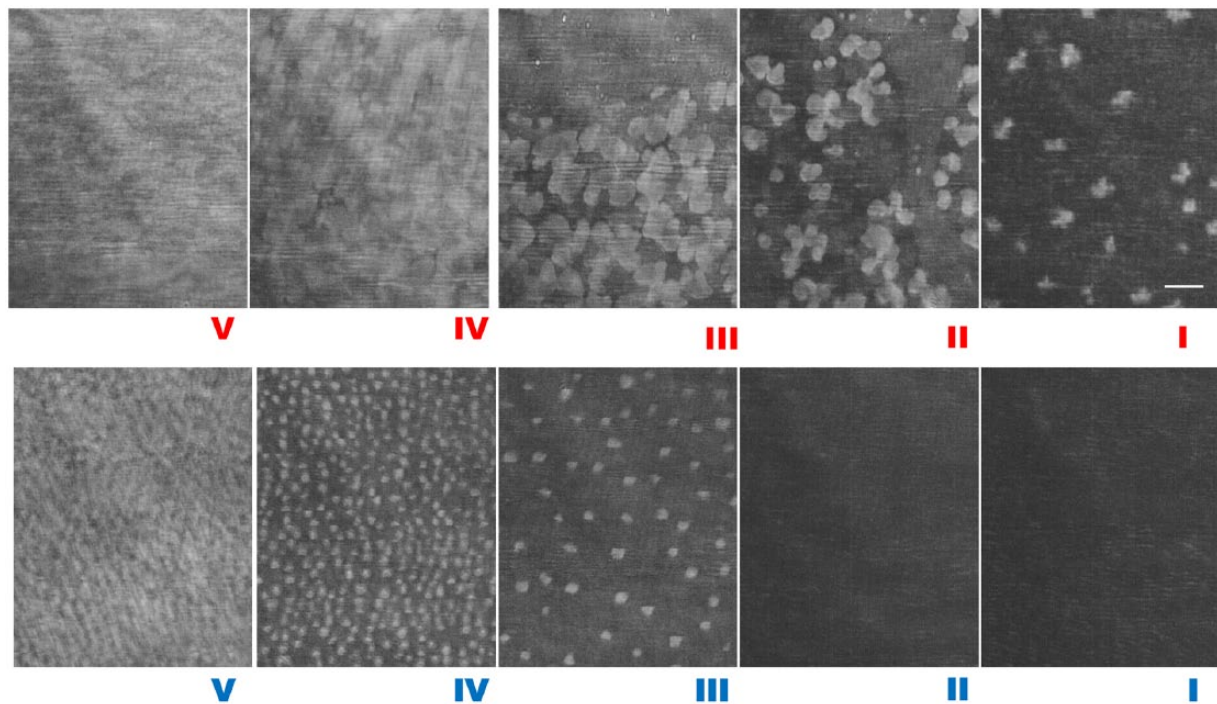
Figure 6. BAM images along compressibility curves of DPPC 11 mM Phe (upper panel) and a mixture of 1:9 DMPC/DPPC (lower panel) (scale bar corresponds to 50 mm). Number corresponds to the peaks shown in Figure 4B.

states of both systems seem comparable regarding curve shape, although it must be noticed that the Phe/DPPC system is shifted to much lower areas and larger pressures in comparison with the Phe/DMPC system (Figure 2A and B, red lines).

According to the K_D values obtained from Figure 1B, Phe affinity is higher in the LE state (DMPC at 33°C). The area increase (Figure 3) implies that Phe molecules may organize around a lipid producing an excluded area larger than that corresponding to pure lipids. This could be explained taking into account that Phe interacts with the lipids by means of H bonds of the defined distance as stated previously.[7] The resulting increased area of this Phe/lipid association leaves less area available for non-bound lipids beyond it that are compelled to condense. This would explain the appearance of small clusters in the Phe/DMPC mixture not observed in DMPC with 10% DPPC.

On the other hand, DPPC in the LC phase may present a coexistence with lipids in the LE state, producing defects of packing, which most probably are in an expanded state. Phe would first occupy these vacancies due to its higher affinity for fluid phases (Figure 1B),[11] promoting the moderate area decrease observed at low concentrations of Phe (Figure 3) due to a decrease in the repulsion forces of lipids in the defect. One possibility would be that Phe occupies the defects due to hydrophobic interactions[7,13] producing a local condensation (area decrease) that results in a larger area available for lipids beyond the occupied defect.

Probably, Phe causes a new Phe phase in DMPC and DPPC monolayers because the Phe/Phospholipid compressibility curves look very similar for both lipids (red lines in Figures 2A

and B and 4A and B). This implies that Phe imposes new arrangements in the lipid phase to form new structures at a high degree of coverage as shown by the binding isotherms in Figure 1. The observation that Phe produces different effects depending on the lipids are in the LE or in the LC state is somehow comparable with the effect of cholesterol that promotes the condensation of LE and expansion of LC phase without affecting the phase transition temperature.[34]

A procedure that allows to analyze the composition of the phases is the deconvolution of the peaks obtained from the derivative of the surface pressure/area per molecule curves.[35] The deconvolution method is applied to samples of 11 mM Phe/DMPC (Figure 7A) and 9:1 molar ratio of the DMPC/ DPPC mixture (Figure 7B). The peaks centered at 184 (Figure 7A) and 70 Å² (Figure 7B) would correspond to the state of maximum compressibility of the monolayer. From the asymmetry of the analyzed peaks, it is inferred that the phase transition would present at least 2 steps corresponding to different molecular orientations in the lipid headgroup region. The deconvolution analysis of the Phe DPPC system (Figure 8A) shows a broad peak centered at approximately 100 Å² comparable with one of the populations present in 1:9 molar ratio of the DMPC/DPPC mixture (Figure 8B). In this case, the 2 populations appear to be in the same range of area.

As observed in Figure 3, the increase in the area per lipid produced in LE DMPC can be explained considering that the association of Phe with lipids results in an increase of regions exposed to water having important consequences on the compressibility properties of domain populations. As denoted by the component analysis of the compressibility
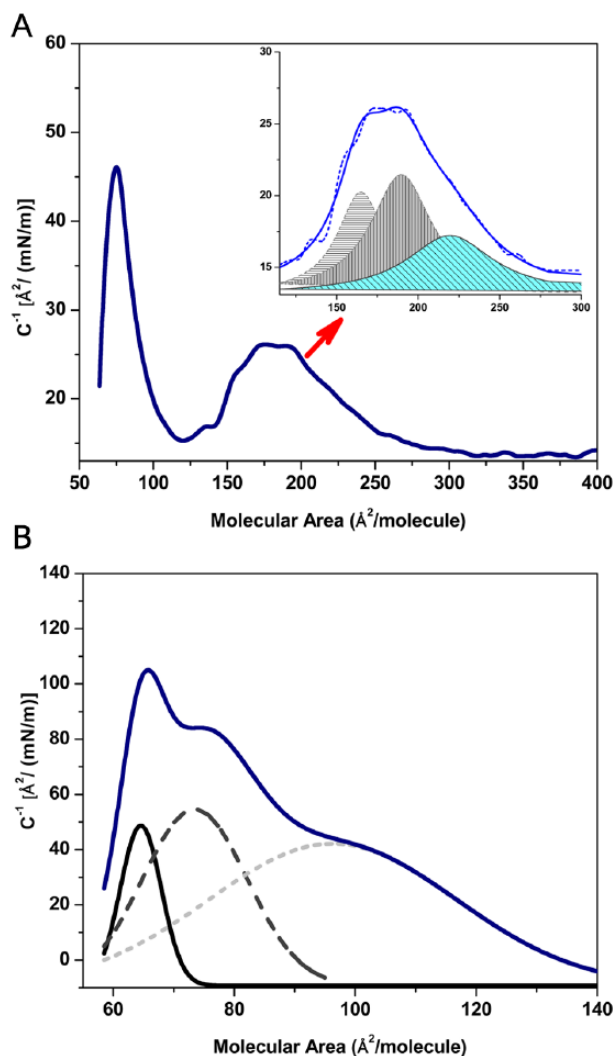
Figure 7. The compressibility curve of 11 mM Phe/DMPC (A) runs from 65 to 450 Å² where 2 main bands were observed at 76.4 (defined band) and 184 Å² (broad band), respectively, and of 9:1 molar ratio of the DMPC/DPPC mixture (B). Inset in (A): the broad band was analyzed applying the deconvolution method. The full blue line is the result of the smoothing and fitting procedure of the experiment (dotted lines) corresponding to the main peak centered at 184 Å² and the 3 components of deconvolution.

Figure 8. Compressibility curves of DPPC/11mM Phe of compressibility module vs area per lipid (A) and of DMPC/DPPC 9:1 mixture (B). Deconvolution was applied in the range of surface pressure between 60 and 110 A2 per molecule (Gray and dashed regions in A and B).

peaks by deconvolution, lateral phase equilibria in multicomponent lipid membranes imply the existence of microscopic regions in the macroscopic phase that present singularities in the membrane topology (defects) or intercalation (partition/solubilization) in the expanded phase promoting changes in macroscopic domains.

Regions of different surface tension on the cell membrane surface can induce changes in the cell shape and can even cause membrane rupture. It is well known that the change in surface tension can have significant consequences for the stability and morphology of a cell membrane.[36,37]

Cell membranes are composed of lipid mixtures that may coexist in domains in the LE and LC states as a result of the composition in sat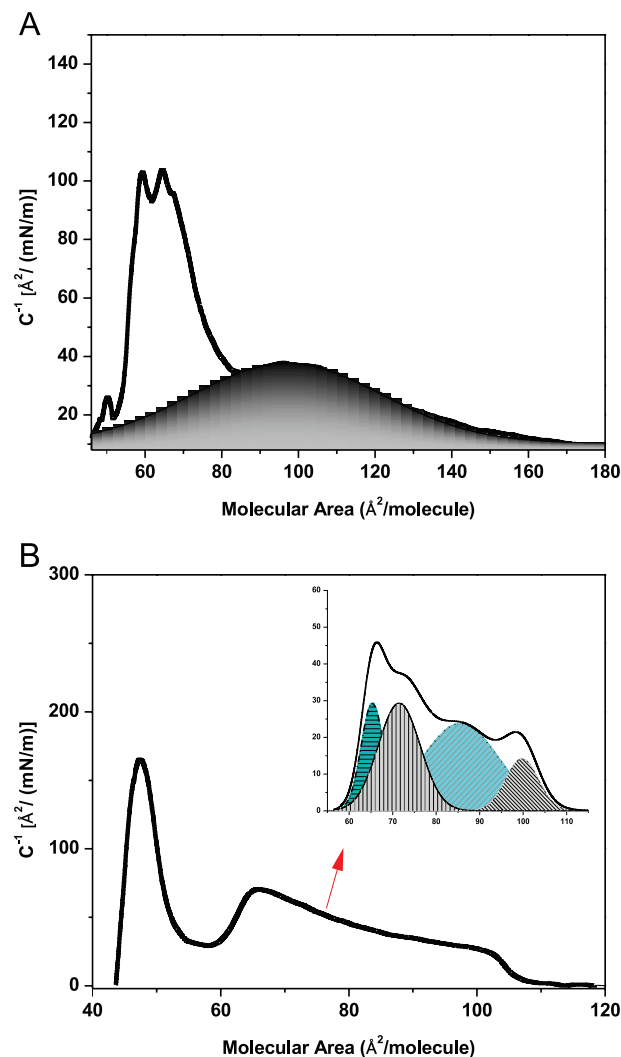urated and unsaturated lipids, cholesterol, and proteins.[21,38] Thus, the action of molecules in the water phase may have a different response, according to its affinity to each of those phases and the interdomain line tension.

In the present case, it is observed that Phe produces effects on lipids in the LE or in the LC state with different affinities.

These effects are somehow comparable with the effect of cholesterol on DPPC monolayers[39] and mixtures of DOPC/DPPC.[29] This effect of Phe on LE and LC monolayers suggests that in a membrane in which both phases coexist cross changes between domains could occur leading to some kind of homeostasis. Due to the different compressibility contribution of each phase in contact with Phe and the decrease in surface tension (increase in surface pressure) induced by the presence of Phe in the interfacial region, the effects on cytotoxicity as well as the change in cell morphology observed might be related to the different capability of deformation.[38,40]

Conclusions

The results of this work show that Phe is able to interact with different affinities in condensed and expanded membranes concurring in a similar final state. Interaction of Phe with the LC and LE phases gives rise to a process in which a synergistic effect between non-independent sites can be produced. The synergism could be explained by the dynamics of microdomains induced by Phe on the nearest neighbors. These features of Phe/lipid interaction would be of great importance to understand the multiple effects of Phe on cell membranes and physiological responses.[1,40]

Author Contributions

A.C.C. was in charge of the BAM images and surface pressure curves. E.A.D. contributed to general discussion. The three authors participated in a mancomunated way in the design and content of the paper. M.A.F. was in charge of the deconvolution analysis, contributed in general discussion and writting of the paper.

Supplemental Material

Supplemental material for this article is available online.

REFERENCES

1. Adler-Abramovich L, Vaks L, Carny O, et al. Phenylalanine assembly into toxic fibrils suggests amyloid etiology in phenylketonuria. *Nat Chem Biol*. 2012;8:701–706.
2. Griffith EC, Perkins RJ, Telesford DM, et al. Interaction of L-phenylalanine with a phospholipid monolayer at the water–air interface. *J Phys Chem B*. 2014;119:9038–9048.
3. Perkins R, Vaida V. Phenylalanine increases membrane permeability. *J Am Chem Soc*. 2017;139:14388–14391.
4. Chiti F, Dobson CM. Protein misfolding, functional amyloid, and human disease. *Annu Rev Biochem*. 2006;75:333–366.
5. Do TD, Kincannon WM, Bowers MT. Phenylalanine oligomers and fibrils: the mechanism of assembly and the importance of tetramers and counterions. *J Am Chem Soc*. 2015;137:10080–10083.
6. Popova AV, Heyer AG, Hincha DK. Differential destabilization of membranes by tryptophan and phenylalanine during freezing: the roles of lipid composition and membrane fusion. *Biochim Biophys Acta*. 2002;1561:109–118.
7. Rosa AS, Cutro AC, Frias MA, Disalvo EA. Interaction of Phenylalanine with DPPC model membranes: more than a hydrophobic interaction. *J Phys Chem B*. 2015;119:15844–15847.
8. Sarangi NK, Ramesh N, Patnaik A. Structure and dynamics of H2O vis-á-vis phenylalanine recognition at a DPPC lipid membrane via interfacial H-bond types: insights from polarized FT-IRRAS and ADMP simulations. *J Chem Phys*. 2015;142:024702.
9. German HW, Uyaver S, Hansmann U. Self-assembly of phenylalanine-based molecules. *J Phys Chem A*. 2014;119:1609–1615.
10. Perkins RJ, Kukharchuk A, Delcroix P, et al. The partitioning of small aromatic molecules to air–water and phospholipid interfaces mediated by non-hydrophobic interactions. *J Phys Chem B*. 2016;120:7408–7422.
11. Cutro AC, Hollmann A, Cejas J, Maturana P, Disalvo EA, Frias MA. Phenylalanine interaction with lipid monolayers at different pHs. *Colloids Surf B Biointerfaces*. 2015;135:504–509.
12. Disalvo EA, Bouchet AM, Frias MA. Connected and isolated CH2 populations in acyl chains and its relation to pockets of confined water in lipid membranes as observed by FTIR spectrometry. *Biochim Biophys Acta*. 2013;1828:1683–1689.
13. Cutro AC, Disalvo EA. Phenylalanine blocks defects induced in gel lipid membranes by osmotic stress. *J Phys Chem*. 2015;119:10060–10065.
14. Avdeef A. pH-metric log P. II: refinement of partition coefficients and ionization constants of multiprotic substances. *J Pharmaceut Sci*. 1993;82:183–190.
15. Raine D, Norris V. Lipid domain boundaries as prebiotic catalysts of peptide bond formation. *J Theoret Biol*. 2007;246:176–185.
16. Netz RR, Andelman D, Orland H. Protein adsorption on lipid monolayers at their coexistence region. *J Physique II*. 1996;6:1023–1047.
17. Alarcón L, de Oca JM, Accordino S, Fris JR, Appignanesi G. Hydrophobicity and geometry: water at curved graphitic-like surfaces and within model pores in self-assembled monolayers. *Fluid Phase Equilibria*. 2014;362:81–86.
18. Alarcón LM, de los Angeles Frías M, Morini MA, Sierra MB, Appignanesi GA, Disalvo EA. Water populations in restricted environments of lipid membrane interphases. *Eur Phys J E*. 2016;39:94.
19. Disalvo EA, Hollmann A, Semorile L, Martini MF. Evaluation of the Defay-Prigogine model for the membrane interphase in relation to biological response in membrane-protein interactions. *Biochim Biophys Acta*. 2013;1828:1834–1839.
20. Disalvo EA, Lairion F, Martini F, et al. Structural and functional properties of hydration and confined water in membrane interfaces. *Biochim Biophys Acta*. 2008;1778:2655–2670.
21. Meder D, Moreno MJ, Verkade P, Vaz WL, Simons K. Phase coexistence and connectivity in the apical membrane of polarized epithelial cells. *Proc Nat Acad Sci U S A*. 2006;103:329–334.
22. Singh V, Rai RK, Arora A, Sinha N, Thakur AK. Therapeutic implication of L-phenylalanine aggregation mechanism and its modulation by D-phenylalanine in phenylketonuria. *Sci Rep*. 2014;4:3875.
23. Baszkin A, Norde W. *Physical Chemistry of Biological Interfaces*. New York, NY: CRC Press; 1999.
24. Fanani ML, Maggio B. Phase state and surface topography of palmitoyl-ceramide monolayers. *Chem Phys Lipids*. 2010;163:594–600.
25. Norde W. *Physical Chemistry of Biological Interfaces*. Baszkin A, Norde W, eds. New York, NY: Marcel Dekker; 2000.
26. Vollhardt D. Brewster angle microscopy: a preferential method for mesoscopic characterization of monolayers at the air/water interface. *Curr Opin Colloid Interface Sci*. 2014;19:183–197.
27. Adamson AWG, Gast AP. *Physical Chemistry of Surface*. (3rd Ed.), Arthur W. Adamson, eds. New York, NY: Wiley-Interscience; 1976.
28. Disalvo EA, Martini MF, Bouchet AM, Hollmann A, Frias MA. Structural and thermodynamic properties of water-membrane interphases: significance for peptide/membrane interactions. *Adv Colloid Interface Sci*. 2014;211:17–33.
29. Qiao L, Ge A, Osawa M, Ye S. Structure and stability studies of mixed monolayers of saturated and unsaturated phospholipids under low-level ozone. *Phys Chem Chemical Phys*. 2013;15:17775–17785.
30. Vollhardt D, Fainerman V. Progress in characterization of Langmuir monolayers by consideration of compressibility. *Adv Colloid Interface Sci*. 2006;127:83–97.
31. Carrer DC, Maggio B. Phase behavior and molecular interactions in mixtures of ceramide with dipalmitoylphosphatidylcholine. *J Lipid Res*. 1999;40:1978–1989.
32. Kjaer K, Kjaer K, Als-Nielsen J, Helm CA, Tippman-Krayer P, Moehwald H. Synchrotron x-ray diffraction and reflection studies of arachidic acid monolayers at the air-water interface. *J Phys Chem*. 1989;93:3200–3206.
33. Honig D, Overbeck GA, Mobius D. Morphology of pentadecanoic acid monolayers at the air/water interface studied by BAM. *Adv Mater*. 1992;4:419–424.
34. Baret J, Hasmonay H, Firpo J, Dupin J, Dupeyrat M. The different types of isotherm exhibited by insoluble fatty acid monolayers. A theoretical interpretation of phase transitions in the condensed state. *Chem Phys Lipids*. 1982;30:177–187.
35. Yu ZW, Jin J, Cao Y. Characterization of the liquid-expanded to liquid-condensed phase transition of monolayers by means of compressibility. *Langmuir*. 2002;18:4530–4531.
36. López-Montero I, Vélez M, Devaux PF. Surface tension induced by sphingomyelin to ceramide conversion in lipid membranes. *Biochim Biophys Acta*. 2007;1768:553–561.
37. Dolowy K. Effect of interfacial tension and curvature of charged lipid bilayer-polylysine complexes. *J Electroanal Chem Interfacial Electrochem*. 1979;104:305–307.
38. Sriram I, Schwartz DK. Line tension between coexisting phases in monolayers and bilayers of amphiphilic molecules. *Surface Sci Rep*. 2012;67:143–159.
39. Gong K, Feng SS, Go ML, Soew PH. Effects of pH on the stability and compressibility of DPPC/cholesterol monolayers at the air–water interface. *Colloids Surf A*. 2002;207:113–125.
40. Birdi K. *Self-Assembly Monolayer Structures of Lipids and Macromolecules at Interfaces*. London, England: Springer; 2006.